JACS
JOURNAL OF THE AMERICAN CHEMICAL SOCIETY
Article
pubs.acs.org/JACS

Dihydrogen Binding to Isostructural $S = {}^1/_2$ and $S = 0$ Cobalt Complexes

Daniel L. M. Suess, Charlene Tsay, and Jonas C. Peters*

Division of Chemistry and Chemical Engineering, California Institute of Technology, Pasadena, California 91125, United States

Supporting Information

ABSTRACT: Two isostructural, nonclassical $Co(H_2)$ complexes are prepared from their $Co(N_2)$ precursors using tris(phosphino)silyl and tris(phosphino)borane ancillary ligands. Comproportionation of $CoBr_2$ and Co metal in the presence of TPB (tris-(*o*-diisopropylphophinophenyl)borane) gives (TPB)-CoBr (**4**). One-electron reduction of **4** triggers N_2 binding to give (TPB)$Co(N_2)$ (**2**-N_2) which is isostructural to previously reported $[SiP_3]Co(N_2)$ (**1**-N_2) ($[SiP_3]$ = tris-(*o*-diisopropylphosphinophenyl)silyl). Both **1**-N_2 and **2**-N_2 react with 1 atm H_2 to generate thermally stable H_2 complexes **1**-H_2 and **2**-H_2, respectively. Both complexes are characterized by a suite of spectroscopic techniques in solution and by X-ray crystallography. The H_2 and N_2 ligands in **2**-H_2 and **2**-N_2 are labile under ambient conditions and the binding equilibria are observable by temperature-dependent UV/vis. A van't Hoff analysis allows for the ligand binding energetics to be determined (H_2: $\Delta H^\circ = -12.5(3)$ kcal mol^{-1} and $\Delta S^\circ = -26(3)$ cal K^{-1} mol^{-1}; N_2: $\Delta H^\circ = -13.9(7)$ kcal mol^{-1} and $\Delta S^\circ = -32(5)$ cal K^{-1} mol^{-1}).

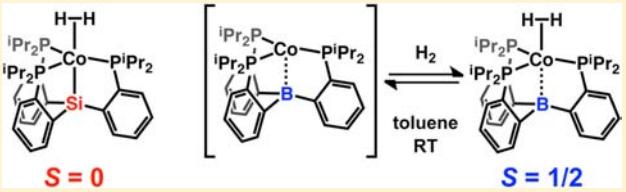

INTRODUCTION

Cobalt-based coordination compounds are active catalysts for a number of H_2-producing and -consuming reactions, including H^+ reduction,[1] H_2 storage,[2] and hydroformylation.[3] In each of these processes, nonclassical $Co(H_2)$ complexes are probable intermediates, and H_2 binding (or release) is likely an elementary mechanistic step. For example, interest in developing earth-abundant catalysts for H^+ reduction has prompted mechanistic investigations of several Co-based catalysts.[4] The three most plausible mechanisms (Scheme 1)

Scheme 1

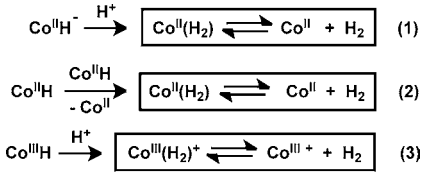

Note: charges are shown for bookkeeping purposes only.

invoke H_2 release from a transient $Co(H_2)$ complex formed by protonation of a Co(II)H species (1), bimolecular coupling of two Co(II)H species (2), or protonation of a Co(III)H species (3). Although mechanisms (1) and (2) employ an $S = {}^1/_2$ $Co(H_2)$ complex, such a complex has never been observed. In fact, reports of open-shell metal dihydrogen complexes are scant.[5,6] There are a few reports of closed-shell $Co(H_2)$ complexes[7,8] (Figure 1); in each case, the complexes' thermal instability called for in situ characterization at low temperature. In addition, the energetics of H_2 binding to Co in any spin state

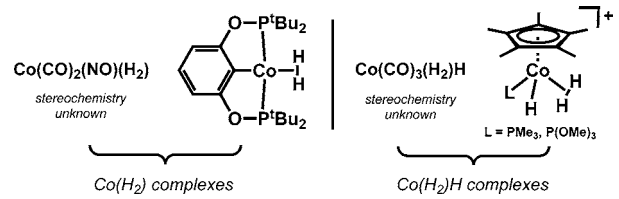

Figure 1. Previously reported $Co(H_2)$ and $Co(H_2)H$ complexes.

or to any homogeneous, open-shell metal complex have not been experimentally ascertained. Given the broad scope of current research interest in the hydrogen chemistry of cobalt, we sought to develop model systems that fill this void. This work presents solution-state and structural studies of a pair of isostructural $Co(H_2)$ complexes in two spin states, including the first example of an $S = {}^1/_2$ $Co(H_2)$ complex. The thermal stability of the complexes allowed for single crystal X-ray diffraction[9] and equilibrium binding studies that are the first of their kind for well-characterized $Co(H_2)$ complexes.

Homogeneous Co complexes with hard donors are not known to form stable H_2 complexes. In contrast, the recently reported $S = 0$ nonclassical $Co(H_2)$ complex (pocop)$Co(H_2)$ (pocop = κ^3-C_6H_3-1,3-$[OP(^tBu)_2]_2$)[7e] is stable in solution below 220 K and is supported by soft, polarizable phosphines; this feature likely promotes low-temperature H_2 binding and thwarts degradative pathways such as oxidative addition or heterolytic cleavage. In addition, its square planar geometry allows it to react with >1 equiv H_2. With these hypotheses in

Received: May 30, 2012
Published: August 14, 2012

   dx.doi.org/10.1021/ja305248f | J. Am. Chem. Soc. 2012, 134, 14158–14164

Scheme 2

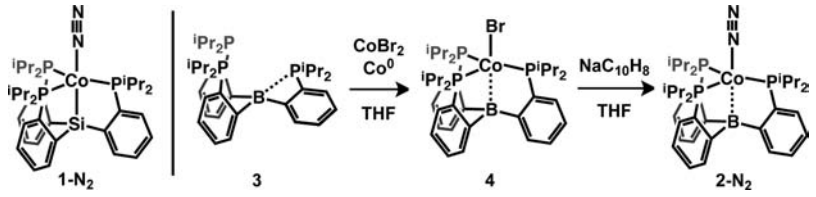

mind, we targeted highly covalent Co fragments of coordination number >3 in order to generate thermally robust Co(H_2) complexes. In particular, we utilize two tetradentate ligands: neutral TPB (tris-(*o*-diisopropylphophinophenyl)borane), introduced by Bourissou,[10] and anionic SiP_3 tris-(*o*-diisopropylphosphinophenyl)silyl), introduced by our lab.[11] Group 10 complexes of the latter ligand have been demonstrated to bind weak σ-donors including H_2 and N_2 while providing minimal activation via π-backbonding.[12]

RESULTS AND DISCUSSION

Preparation of Co(N_2) Synthons. We previously reported the S = 0 [SiP_3]Co(N_2) complex (**1**-N_2)[11] and targeted the isostructural complex (TPB)Co(N_2) (**2**-N_2) as a precursor to an $S = {}^1/_2$ Co(H_2) species. Installation of Co into TPB (**3**) was accomplished by metalation with $CoBr_2$ in the presence of excess Co powder (Scheme 2). Orange-brown (TPB)CoBr (**4**) has a solution magnetic moment of μ_{eff} = 3.0 μ_B (298 K), consistent with an S = 1 spin state. Its solid-state geometry is between tetrahedral and trigonal bipyramidal with a Co−B distance of 2.4629(8) Å (Figure 2). Thus, **4** can be viewed analogously to Thomas's Co−Zr heterobimetallic complexes supported by phosphinoamide ligands.[13]

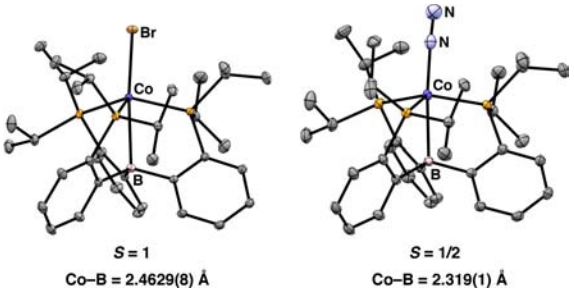

Figure 2. Solid-state structures of **4** (left) and **2**-N_2 (right). H atoms are omitted for clarity and thermal ellipsoids are drawn at the 50% probability level.

Reduction of **4** with $NaC_{10}H_8$ under N_2 yields yellow, $S = {}^1/_2$ (TPB)Co(N_2) (**2**-N_2; μ_{eff} = 1.5 μ_B, 298 K). Its EPR spectrum shows a nearly axial signal (**g** = [2.561, 2.077, 2.015]) (Figure 3, top). In the solid state, **2**-N_2 adopts a trigonal bipyramidal geometry with a Co−B bond length of 2.319(1) Å (Figure 2). The N_2 ligand of **2**-N_2 is labile in solution as well as in the solid state (*vide infra*). An intense $\nu_{(N-N)}$ stretch is observed by IR spectroscopy at 2089 cm^{-1}. Compared with isostructural **2**-N_2, **1**-N_2 has one additional valence electron and has a correspondingly lower $\nu_{(N-N)}$ IR stretch of 2063 cm^{-1}.[11,14] A similar $\nu_{(N-N)}$ stretch (2081 cm^{-1}) has been recently reported for a topologically related cobalt alatrane complex.[15]

Characterization of [SiP_3]Co(H_2) and (TPB)Co(H_2). Although **1**-N_2 is stable to vacuum in solution, it converts over several hours to **1**-H_2 under 1 atm H_2 at RT (Scheme 3).

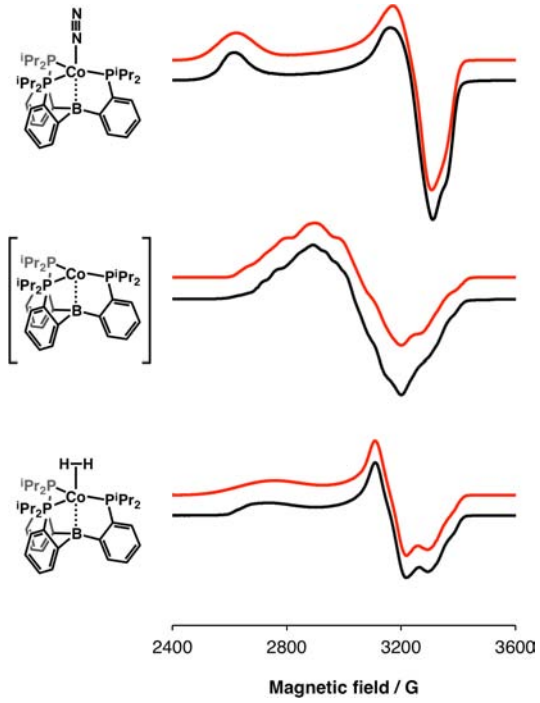

Figure 3. EPR spectra of **2**-N_2 (top), **2** (middle), and **2**-H_2 (bottom) recorded in toluene glass at 10 K and 9.38 GHz. Black traces: experiment; red traces: simulation.

Scheme 3

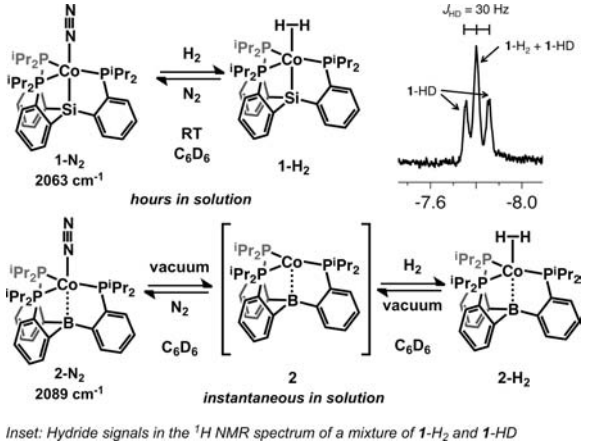

Both **1**-H_2 and **1**-N_2 are orange and exhibit a single sharp resonance in their ^{31}P NMR spectra (79.8 and 65.6 ppm, respectively), consistent with a C_3-symmetric structure in solution. The ^1H NMR signals for the dihydrogen ligands of **1**-H_2 and **1**-HD appear at −7.78 ppm and −7.80 ppm (J_{HD} = 30 Hz), respectively (Scheme 3 inset). Temperature-dependent T_1 relaxation studies reveal T_1(min) = 29 ms (243 K, 500 MHz). The high J_{HD} coupling constant and low T_1(min) value support

dx.doi.org/10.1021/ja305248f | J. Am. Chem. Soc. 2012, 134, 14158−14164

the formulation of **1**-H_2 as a nonclassical H_2 complex rather than a dihydride in solution.[16]

Although **1**-H_2 is indefinitely stable in solution at RT under an H_2 atmosphere, **1**-N_2 is slowly formed upon exposure of **1**-H_2 to 1 atm N_2. The thermal stability of **1**-H_2 allowed us to obtain high-quality single crystals for an X-ray structure determination (Figure 4). The data reveal a coordination

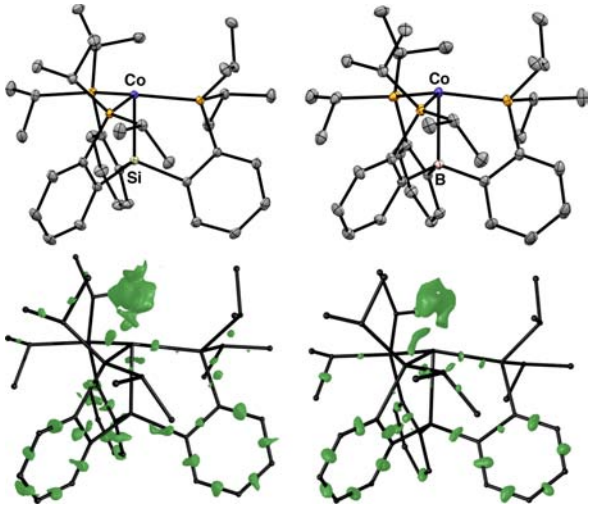

Figure 4. Solid-state structures of **1**-H_2 (top, left) and **2**-H_2 (top, right). H atoms are omitted for clarity, and thermal ellipsoids are drawn at the 50% probability level. Positive residual electron density isosurfaces of **1**-H_2 (bottom, left) and **2**-H_2 (bottom, right) drawn at the +0.47 electrons $Å^{-3}$ level.

geometry of approximately C_3 symmetry with Co−P and Co−Si distances slightly shorter than those observed in **1**-N_2. The apical H_2 ligand could not be located in the difference map, though a globular disk of residual electron density is observed (*vide infra*).

Unlike for **1**-N_2, application of vacuum to a toluene solution of **2**-N_2 results in formation of a new species. Dark brown **2** absorbs more strongly than **2**-N_2 in the entire visible region, with the former having characteristic absorption bands at 510 and 806 nm (ε = 640 and 690 M^{-1} cm^{-1}, respectively). This transformation can be observed by ^{1}H NMR spectroscopy; **2**-N_2 and **2** show different sets of 10 paramagnetically shifted signals, indicating that both species are C_3-symmetric in solution. The EPR spectrum of **2** (Figure 3, middle) shows the disappearance of the signal corresponding to **2**-N_2 as well as a new signal (g = [2.372, 2.166, 2.089]). Attempts to grow single crystals of **2** under Ar or vacuum have been unsuccessful. There are several reasonable structures of **2**: (i) a dicobalt bridging N_2 complex of the form (TPB)Co-(μ-1,2-N_2)-Co(TPB); (ii) a cyclometalated species under rapid exchange in which a ligand C−H bond has been intramolecularly activated; (iii) a trigonal pyramidal species with a vacant site trans to the B atom; (iv) a complex with either a weak intramolecular agostic interaction or bound solvent molecule. The solution Raman spectrum of **2** does not display any resonances between 1700 and 2300 cm^{-1}, the region in which $\nu_{(N-N)}$ and $\nu_{(Co-H)}$ stretches are anticipated. This leads us to favor structural possibilities (iii) or (iv) rather than (i) or (ii). Additionally, **2** may be formed in arene (benzene and toluene) as well as more weakly coordinating solvents (pentane and HMDSO); this leads us to disfavor solvent binding. Structure-type (iii) has been previously observed for the related trigonal pyramidal complexes of $[SiP_3]$[12b] and (TPB).[17] The optimized geometry of **2** (B3LYP) reveals a trigonal pyramidal geometry of structure-type (iii) and a short Co−B distance of 2.14 Å; attempts to locate a minimum geometry with an intramolecular C−H agostic interaction resulted in convergence to structure-type (iii) (see SI).

Addition of H_2 to solutions of **2** results in new spectroscopic features that are most consistent with formation of the nonclassical H_2 complex **2**-H_2. In solution under 1 atm H_2, the UV/vis spectrum of **2**-H_2 is similar to that of **2**-N_2. The ^{1}H NMR spectrum of **2**-H_2 under 1 atm H_2 consists of 10 paramagnetically shifted signals, indicating that **2**-H_2 is C_3-symmetric on the NMR time scale. In addition, no peak corresponding to free H_2 is observed at room temperature, suggesting that H_2 is interacting rapidly with **2** (a sharp peak corresponding to free H_2 is not observed above −90 °C in toluene-d^8). The EPR spectra of **2**-H_2 and **2**-N_2 are similar, with the former exhibiting somewhat greater rhombicity as displayed by its more pronounced splitting of g_2 and g_3 (Figure 3, bottom; g = [2.457, 2.123, 2.029]). The EPR spectra of **2**-H_2 and **2**-D_2 are identical (see SI) and broad; as a result, no ^{1}H hyperfine coupling can be gleaned. Raman spectra of **2**-H_2 and **2**-D_2 (in both solution and solid states) are identical; this observation precludes the presence of Co−H(D) bonds in **2**-$H_2(D_2)$ which are expected to have observable stretches that are subject to isotopic shifts approximated by the harmonic oscillator model. In contrast to M−H(D) stretches, H−H and D−D stretches often are too weak to observe or are obscured by resonances attributed to the other ligands.[5a,6]

Orange single crystals of **2**-H_2 were grown by slowly cooling a saturated solution of **2**-H_2 under 1 atm H_2. The sample diffracted strongly to 0.58 Å, and the final solution (not including the H_2 ligand) fits the data very satisfactorily (see SI). The (TPB)Co frameworks of **2**-N_2 and **2**-H_2 are similar, with the latter exhibiting slightly contracted Co−P and Co−B bonds (Figure 4 and Table 1). The analogous contraction in Co−P and Co−Si bond lengths also occurs between **1**-H_2 and **1**-N_2. Akin to **1**-H_2, a globular disk of residual positive electron density trans to the B atom is observed. The irregular shape may arise from static positional disorder of the H_2 ligand or from dynamic tunneling between states separated by the rotational barrier of the H_2 ligand as was postulated for the related complex $[SiP_3]Fe(H_2)$ **5**-H_2.[6] A similarly shaped surface of the residual electron density is generated from the X-ray data of **5**-H_2 (see SI).

Table 1. Selected Bond Lengths and Angles

	1-N_2	**1**-H_2	**2**-N_2	**2**-H_2
Co−P/Å	2.2277(6)	2.1933(2)	2.2600(4)	2.2412(3)
	2.2342(7)	2.2027(2)	2.2655(4)	2.2650(3)
	2.2376(6)	2.2029(2)	2.3288(4)	2.2750(3)
P−Co−P/Å	119.51(2)	119.58(1)	128.79(1)	124.49(1)
	118.01(2)	119.11(1)	112.22(1)	119.00(1)
	117.48(2)	117.52(1)	107.87(1)	110.97(1)
Co−Si/Å	2.2327(7)	2.2048(3)		
Co−B/Å			2.319(1)	2.280(1)

The non-H atom locations of **2**-H_2 provide further support for formulating **2**-H_2 as an H_2 complex rather than a dihydride. In particular, an octahedral *cis*-dihydride is expected to exhibit one wide P−Co−P angle to accommodate a bisecting hydride

dx.doi.org/10.1021/ja305248f | J. Am. Chem. Soc. 2012, 134, 14158−14164

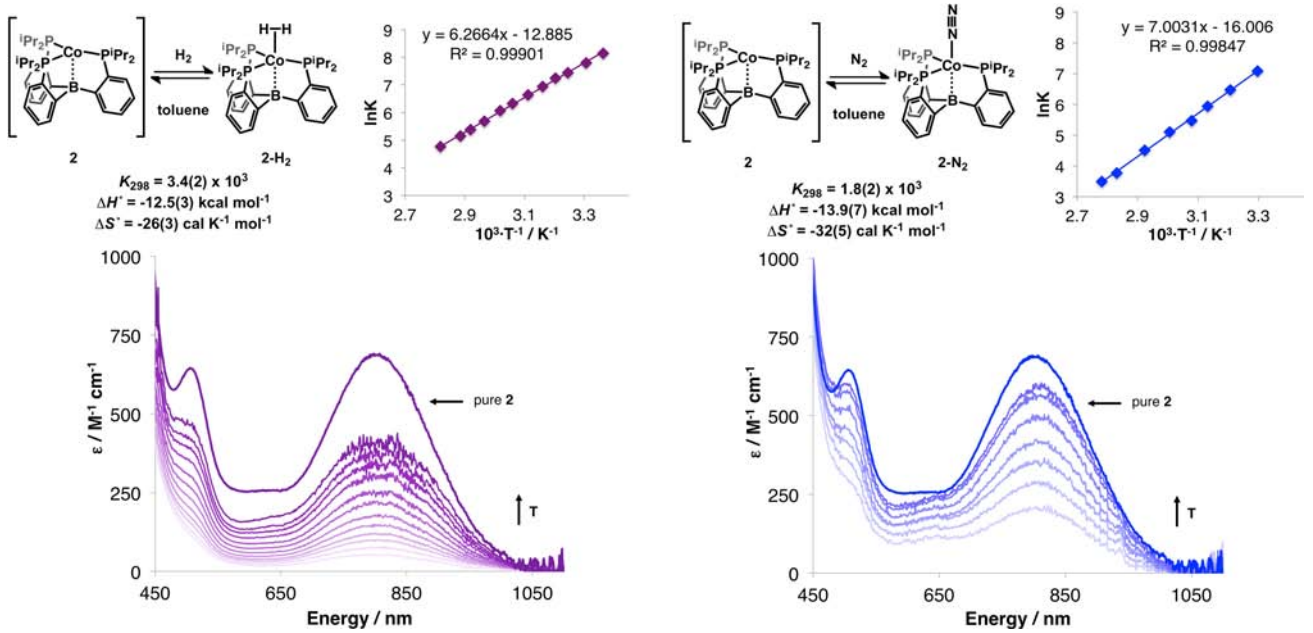

Figure 5. Temperature-dependent UV/vis studies of H_2 (left) and N_2 (right) binding to **2** in toluene under 1 atm H_2 or N_2. The top traces in the UV/vis spectra are pure **2** in toluene under vacuum. Darker traces correspond to higher temperatures. Van't Hoff plots of the equilibrium of H_2 or N_2 binding to **2** are derived from monitoring the concentration of **2** as indicated by the absorbance at 740 nm (see Experimental Section). The standard states for **2**, **2**-H_2, **2**-N_2, H_2, and N_2 are defined as 1 M in toluene for all species at 25 °C. Caution should be exercised in directly comparing these thermodynamic values since the standard states may be defined differently.

ligand. The widest P−Co−P angle in **2**-H_2 is 124.49(1)° which is significantly narrower than would be expected.[18] Alternatively, if the H−H bond is cleaved in **2**-H_2 to give a trigonal bipyramidal species of the form Co(H)(TPB-H), the boron in **2**-H_2 would be expected to be tetrahedral with nearly linear B−H−Co bonding; this isomer would have a significantly longer Co−B distance than what is observed. The non-H atom positions in the DFT-optimized structure (see SI) are consistent with the X-ray structure; the intact H_2 ligand in the optimized structure is not significantly elongated compared with free H_2 (0.82 and 0.74 Å, respectively).

Although the spectroscopic and computational data support the formulations of **1**-H_2 and **2**-H_2 as nonclassical H_2 complexes, it remains possible that dihydride structures and/or a hydride−borohydride structure for **2**-H_2 are thermally accessible. We have observed reversible H_2 activation across a M−B bond in a related diphosphinoborane nickel systems to form a (B−H)Ni(H) motif.[19] Both **1**-H_2 and **2**-H_2 facilitate scrambling of HD to give H_2, D_2, and HD; although this process may be mediated by transient hydrido species, it may also be accomplished by other conceivable mechanisms such as Lewis acidic H_2 activation and deprotonation by trace exogenous base.

Thermochemistry of H_2 and N_2 Binding to 2. The lability of N_2 and H_2 from **2**-N_2 and **2**-H_2 under vacuum contrasts with the behavior of **1**-N_2 and **1**-H_2 (both of which are stable to vacuum). Additionally, the UV/vis spectra of **2**-N_2 and **2**-H_2 (1 atm N_2 or H_2, toluene, RT) show a small quantity of **2** which is readily identified by its characteristic band at 806 nm. This subtle feature prompted us to study the thermochemistry of H_2 and N_2 binding to **2** by UV/vis spectroscopy.

Gratifyingly, the temperature dependence of K_{H2} could be extracted by monitoring the concentration of **2** by UV/vis spectroscopy in the range 24.2−81.7 °C (toluene, 1 atm H_2; Figure 5, left). A van't Hoff analysis reveals the energetics of H_2 binding to **2**: $\Delta H^\circ = -12.5(3)$ kcal mol^{-1} and $\Delta S^\circ = -26(3)$ cal K^{-1} mol^{-1}. These values may include contributions from a weak agostic interaction or interaction with solvent, depending on the solution structure of **2** (*vide supra*). This work is, to our knowledge, the first time the energetics of H_2 binding to a homogeneous Co complex have been determined experimentally. These values are in line with representative examples of H_2 binding energetics for other homogeneous metal complexes (ΔH°: −6.5 to −18 kcal mol^{-1}; ΔS°: −19 to −44 cal K^{-1} mol^{-1}).[20] Caution should be exercised in directly comparing these thermodynamic values since the standard states may be defined differently.

An analogous study of N_2 binding to **2** was undertaken between 30.2−86.3 °C (toluene, 1 atm N_2; Figure 5, right), and the energetics of N_2 binding to **2** were determined to be $\Delta H^\circ = -13.9(7)$ kcal mol^{-1} and $\Delta S^\circ = -32(5)$ cal K^{-1} mol^{-1}. Compared with N_2, binding H_2 is slightly less favorable enthalpically and less *dis*favorable entropically. The more negative value of ΔS° for N_2 binding is in part due to the higher absolute entropy of free N_2. Similar observations have been made for Cr, Mo, and W complexes.[20a,b,f]

Comparison with Related Trigonal Bipyramidal M(H_2) Complexes. Isostructural **1**-H_2 and **2**-H_2 are themselves rare examples of Co(H_2) complexes and, along with [SiP_3]Fe(H_2) (**5**-H_2) and {[SiP_3]Ni(H_2)}{$BAr^F{}_4$} (**6**-H_2),[12a] constitute a family of (M−E)[9] and (M−E)[10] H_2 complexes that are well-suited for comparison (Table 2).[21] For example, **2**-H_2 and **5**-H_2 are valence isoelectronic, thermally stable complexes. However, the M(H_2) interaction is weaker in **2**-H_2, presumably due to the poorer π-backbonding ability of Co compared with Fe. This difference allows for the equilibrium of N_2 and H_2 binding to **2** to be observed at ambient conditions (1 atm H_2 or N_2 at RT), whereas **5**-N_2 and **5**-H_2 are stable to vacuum. On the other hand, **1**-H_2 and **2**-H_2 are neutral complexes of Co that vary by

dx.doi.org/10.1021/ja305248f | J. Am. Chem. Soc. 2012, 134, 14158−14164

Table 2. Isostructural Trigonal Bipyramidal H_2 Adducts

	$(M-E)^9$	$(M-E)^{10}$
does not lose H_2 under vacuum	$[SiP_3]Fe(H_2)^a$ **5**-H_2	$[SiP_3]Co(H_2)^b$ **1**-H_2
loses H_2 under vacuum	$(TPB)Co(H_2)^b$ **2**-H_2	$\{[SiP_3]Ni(H_2)\}^{+c}$ **6**-H_2

[a]Ref 6. [b]This work. [c]Ref 12a. For **2**-H_2, the H_2 ligand is labile under 1 atm H_2. For **6**-H_2, the H_2 ligand is labile under vacuum.

one valence electron by virtue of their differing main group element. Compared with **2**-H_2, the H_2 binding affinity is enhanced in the more electron-rich **1**-H_2 which is stable to vacuum in the solution and solid states. As a final comparison, the H_2 binding affinity of **1**-H_2 is somewhat tempered in the valence isoelectronic analogue **6**-H_2. Under 1 atm H_2, trigonal pyramidal **6** is fully converted to **6**-H_2; however, the H_2 ligand dissociates upon application of vacuum. The H_2 binding affinity of **6**-H_2 therefore lies somewhere between that of **2**-H_2 and that of **1**-H_2 or **5**-H_2. Thus, the H_2 binding strength may be tuned by adjusting the identity of the M−E unit.

CONCLUSION

In conclusion, a pair of isostructural $Co(H_2)$ complexes have been prepared and characterized. **1**-H_2 and **2**-H_2 are notable for their thermal stability and are the first $Co(H_2)$ complexes to be characterized crystallographically. In addition, **2**-H_2 is the first reported $S = {}^1/_2$ $Co(H_2)$ complex and one of very few well-characterized paramagnetic $M(H_2)$ complexes. The less electron-rich **2**-H_2 binds H_2 (and N_2) less strongly than the $S = 0$ complex **1**-$H_2(N_2)$. This attenuated binding strength allows for the solution equilibrium energetics of H_2 and N_2 binding to **2** to be observed. This work demonstrates that within a family of isostructural $(M-E)^{9,10}$ H_2 complexes, the valence electron count and the H_2 binding affinity may be systematically tuned by adjusting the identity of M and E.

EXPERIMENTAL SECTION

General Considerations. All manipulations were carried out using standard Schlenk or glovebox techniques under an atmosphere of dinitrogen. Solvents were degassed and dried by sparging with N_2 gas and passage through an activated alumina column. Deuterated solvents were purchased from Cambridge Isotopes Laboratories, Inc. and were degassed and stored over activated 3 Å molecular sieves prior to use. Reagents were purchased from commercial vendors and used without further purification unless otherwise noted. **1**-N_2[23] and (TPB)[24] were synthesized according to literature procedures. Elemental analyses were performed by Midwest Microlab (Indianapolis, IN).

Spectroscopic Measurements. ^1H, ^{13}C, and ^{31}P NMR spectra were collected at room temperature, unless otherwise noted, on Varian 300 MHz, 400 MHz, and 500 MHz NMR spectrometers. ^1H and ^{13}C spectra were referenced to residual solvent resonances. ^{31}P spectra were referenced to external 85% phosphoric acid ($\delta = 0$ ppm). T_1(min) values were determined by fitting the pulse-recovery ^1H spectra at various temperatures using the T_1 calculation protocols in either Varian's VnmrJ software or Mestrelab Research S. L.'s Mestrenova version 6.2.1. EPR spectroscopy were recorded on a Bruker EMS spectrometer at ∼1 mM concentrations. IR measurements were obtained in KBr pellets using a Bio-Rad Excalibur FTS 3000 spectrometer with Varian Resolutions Pro software. Solution-state Raman spectra were acquired using a coherent Innova 70 5-W Ar-ion laser, a Spex 750 M spectrograph with a 1200 gr/mm grating, and a Horiba Jobin Yvon Synapse TE cooled CCD detector. Solid-state Raman spectra were acquired on a Renishaw M1000 Micro Raman spectrometer system using an Ar ion laser and 514.5 nm excitation.

X-ray Crystallography. X-ray diffraction studies were carried out at the Caltech Division of Chemistry and Chemical Engineering X-ray Crystallography Facility on a Bruker three-circle SMART diffractometer with a SMART 1K CCD detector. Data were collected at 100 K using Mo Kα radiation (λ = 0.71073 Å). Structures were solved by direct or Patterson methods using *SHELXS* and refined against F^2 on all data by full-matrix least-squares with *SHELXL-97*.[25] All non-hydrogen atoms were refined anisotropically. All hydrogen atoms were placed at geometrically calculated positions and refined using a riding model except for those corresponding to H_2 ligands. The isotropic displacement parameters of all hydrogen atoms were fixed at 1.2 (1.5 for methyl groups) times the Ueq of the atoms to which they are bonded.

Computational Details. All calculations were performed using the *Gaussian03* suite.[26] The geometry optimizations were done without any symmetry restraints at the DFT level of theory using the B3LYP hybrid functional. The 6-31G(d) basis set was used for all atoms. The full ligand was used for each calculation, and the minimized structures were verified with frequency calculations. The starting coordinates for the metal and ligand were taken from the crystal structures. To model H_2 adducts, hydrogen atoms were initially placed in the apical binding site at an arbitrary initial distance of 1.5 Å from the metal and 0.9 Å from each other. To model dihydrides, hydrogen atoms were initially placed orthogonal to one another (one in the apical site and one bisecting a P−M−P angle) at a distance of 1.4 Å from the metal.

Preparation of $[SiP^{iPr}_3]Co(H_2)$ (1-H_2). Under a dinitrogen atmosphere, **1**-N_2 (12 mg, 17 μmol) was dissolved in toluene-d_8, transferred to a J. Young tube, and sealed. The sample was freeze−pump−thawed three times, then exposed to 1 atm H_2 while frozen. No visible change occurred upon thawing the sealed tube. The reaction was complete after five days at room temperature, without agitation; the solution remained orange. The H_2 adduct remained intact through three freeze−pump−thaw cycles, as well as 1.5 h under static vacuum in solution. Exposure to an N_2 atmosphere, however, resulted in gradual displacement of the H_2 and reversion to the starting N_2 adduct. As such, elemental analysis was not performed. Single crystals were grown by slow concentration of a benzene solution. ^1H NMR (toluene-d_8, δ): 8.10 (d, J = 7 Hz, 3H), 7.23 (m, 3H), 7.20 (m, 3H), 7.05 (m, 3H), 2.22 (br s, 6H), 0.94 (s, 18H), 0.49 (br s, 18H), −7.78 (br s, 2H). T_1(min) (−30 °C, 500 MHz) = 29 ms. $^{13}C\{^1H\}$ NMR (toluene-d_8, δ): 157.2 (m), 147.9 (m), 132.4 (m), 128.5 (s), 127.7 (s, partially overlapping with solvent peak), 126.4 (s), 28.1 (br s), 19.2 (s), 18.7 (s). $^{31}P\{^1H\}$ NMR (toluene-d_8, δ): 79.8 (s).

Preparation of $[SiP^{iPr}_3]Co(HD)$ (1-HD). A sample of $[SiP^{iPr}_3]Co(N_2)$ (8 mg, 11 μmol) dissolved in toluene-d_8 in a J. Young tube was freeze−pump−thawed three times, then exposed to ∼1 atm HD (generated from the reaction of excess $LiAlH_4$ and D_2O) while frozen. Upon thawing in the sealed tube and sitting at room temperature for 5 days, the solution remained orange, and the NMR spectra showed complete conversion to the HD adduct. ^1H NMR (toluene-d_8, δ): 8.10 (d, J = 6 Hz, 3H), 7.23 (m, 3H), 7.20 (m, 3H), 7.05 (m, 3H), 2.22 (br s, 6H), 0.94 (s, 18H), 0.49 (br s, 18H), −7.80 (dt, $^1J_{HD}$ = 30 Hz, $^2J_{HP}$ = 6 Hz, 1H). $^{31}P\{^1H\}$ NMR (toluene-d_8, δ): 79.0 (s).

Preparation of (TPB)CoBr (4). A Schlenk tube was charged with TPB (**3**, 502.0 mg, 0.8500 mmol), $CoBr_2$ (185.9 mg, 0.8500 mmol), Co powder (249.6 mg, 4.250 mmol), THF (20 mL), and a magnetic stirbar. The green solution was heated at 90 °C for 2 days. After cooling, the residue was transferred to a 500 mL filter flask in a glovebox. The solvent was removed from the resulting deep yellow-green solution *in vacuo* to give a dark residue. Residual THF was removed by adding benzene (5 mL) to the residue and evaporating to dryness under vacuum. Pentane (200 mL) was added and stirred vigorously for 5 min. This resulted in formation of a yellow solution with blue precipitate. The solution was decanted from the solids and filtered through a pad of Celite on a scintered glass frit. The remaining solids were extracted with pentane (60 mL portions) until the extracts were colorless (four times); the extracts were filtered and combined with the first batch. Removal of the solvent in vacuo provided a yellow-brown solid that was dissolved in benzene (5 mL) and lyophilized to give an orange-brown solid (435 mg, 0.596 mmol, 70%). Single

dx.doi.org/10.1021/ja305248f | J. Am. Chem. Soc. 2012, 134, 14158−14164

crystals were grown by slow evaporation of an Et_2O solution into HMDSO. ^1H NMR (400 MHz, C_6D_6) δ 111.76, 29.58, 16.71, 15.99, 4.59, −0.03, −0.20, −1.01, −2.66, −8.34. Elemental analysis for $C_{36}H_{54}BBrCoP_3$: calc. C 59.28 H 7.46, found C 58.90 H 7.17

Preparation of (TPB)Co(N_2) (2-N_2). A solution of $NaC_{10}H_8$ was prepared by stirring naphthalene (34.3 mg, 0.277 mmol) and sodium (23.7 mg, 1.03 mmol) in THF (3 mL) for 4 h. The resulting deep-green solution was filtered and added dropwise to a stirring solution of **4** (149.4 mg, 0.2056 mmol) in THF (2 mL). The resulting dark red-brown solution was allowed to stir for 6 h. Solvent was removed *in vacuo* and the resulting dark red-brown residue was dissolved in benzene (2 mL). Solvent was again removed *in vacuo*, and the resulting solid was stirred in benzene (3 mL) for 5 min. The brown solution was filtered through a pad of Celite and lyophilized to give dark brown **2**. Solid samples of **2** stored under N_2 turned bright yellow over several days, giving **2**-N_2 (106.0 mg, 0.1566 mmol, 76%). Single crystals were grown by slow evaporation of an Et_2O solution into HMDSO. ^1H NMR (400 MHz, C_6D_6) δ 26.95, 23.82, 16.28, 11.35, 5.09, 2.15, 1.56, −0.60, −1.35, −1.73. Elemental analysis shows low values for N which is consistent with the observed lability of the N_2 ligand.

Generation of "(TPB)Co" 2. A yellow solution of **2**-N_2 in C_6D_6 was subjected to three freeze−pump−thaw cycles which resulted in formation of a dark brown solution. The transformation is clean by ^1H NMR and reversible by exposure to N_2 atmosphere to reform **2**-N_2. ^1H NMR (400 MHz, C_6D_6) δ 59.33, 14.93, 12.96, 10.31, 5.42, 3.88, 1.38, −0.10, −2.05, −3.97. Elemental analysis was not obtained due to the compound's propensity to bind atmospheric N_2.

Generation of (TPB)Co(H_2) (2-H_2). A dark brown solution of **2** under vacuum was exposed to 1 atm H_2, resulting in immediate formation of a yellow solution. The transformation is clean by ^1H NMR and reversible by subjecting the solution to three freeze−pump−thaw cycles to reform **2**. Single crystals were grown by slowly cooling a saturated HMDSO/methylcyclohexane (1:1) solution of **2**-H_2 under 1 atm H_2. ^1H NMR (400 MHz, C_6D_6) δ 27.48, 22.60, 15.17, 10.34, 5.52, 2.75, 1.21, 0.43, −0.84, −2.51. Elemental analysis was not obtained because the compound is only stable to H_2 loss under H_2 atmosphere.

Measurement of $K(H_2)$ As a Function of Temperature. A 0.00390 M solution of **2**-N_2 (23.8 mg, 0.0351 mmol) in toluene (9.00 mL) was generated in a glovebox. A two-necked glass tube with a 24/40 joint on top and a side arm with a 14/20 joint was charged with the solution and a stirbar. The 24/40 joint was equipped with a dip probe (Hellma Worldwide, 10 mm, 661.302-UV model), and the 14/20 joint was fitted with a rubber septum. The septum was pierced with a hole that allowed for introduction of a thermocouple into the solution. The sealed apparatus was removed from the glovebox and connected to a Schlenk line. The solution was frozen, evacuated, and refilled with H_2. This was repeated an additional two times. The UV/vis spectrum was recorded at twelve temperatures, allowing for at least 2 min to equilibrate at each temperature: 24.2, 29.3, 35.0, 39.0, 43.2, 48.2, 53.7, 58.1, 64.1, 69.4, 73.4, and 81.7 °C (see Figure 4 in the main text). The concentration of **2** was calculated from the absorbance at 740 nm based on the known extinction coefficient of a pure sample of **2** at 740 nm (see Figure 4). This wavelength (740 nm) was selected instead of the peak's maximum (806 nm) because of signal saturation around 800 nm that arises from a strong absorbance in the background. The binding constant $K(H_2)$ was calculated at each temperature using the equations:

$$K(H_2) = [\mathbf{2}\text{-}H_2]/([H_2][\mathbf{2}])$$

where

$$[\mathbf{2}\text{-}H_2] = 0.0351/V(\text{tol}) - [\mathbf{2}]$$

The temperature dependence of $[H_2]$ in toluene[27] and the density of toluene were taken from the literature.[28] An identical procedure was undertaken to measure the N_2 binding data using 6.7 mg **2**-N_2 and $[N_2]$ in toluene from the literature.[29]

■ ASSOCIATED CONTENT

Ⓢ Supporting Information

Spectra, computational details, complete ref 26, and X-ray crystallographic information. This material is available free of charge via the Internet at http://pubs.acs.org.

■ AUTHOR INFORMATION

Corresponding Author

jpeters@caltech.edu

Notes

The authors declare no competing financial interest.

■ ACKNOWLEDGMENTS

We thank the Gordon and Betty Moore Foundation and the NSF Center for Chemical Innovation on Solar Fuels (CCI Solar, CHE-0802907 and CHE-0947829) for funding. We thank Prof. George Rossman (solid-state Raman studies), Maraia Ener (solution-state Raman studies), and Lawrence Henling (X-ray crystallography) for experimental assistance.

■ REFERENCES

(1) Recent reviews: (a) Losse, S.; Vos, J. G.; Rau, S. *Coord. Chem. Rev.* **2010**, *254*, 2492−2504. (b) Wang, M.; Chen., L.; Sun, L. *Energy Environ. Sci.* **2012**, advance article.

(2) (a) Dinca, M; Long, J. R. *Angew. Chem., Int. Ed.* **2008**, *47*, 6766−6779. (b) Suh, M. P.; Park, H. J.; Prasad, T. K.; Lim, D.-W. *Chem. Rev.* **2012**, *112*, 782−835.

(3) Hebrard, F.; Kalck, P. *Chem. Rev.* **2009**, *109*, 4272−4282.

(4) Mechanistic possibilities are laid out in the following account: Dempsey, J. L.; Brunschwig, B. S.; Winkler, J. R.; Gray, H. B. *Acc. Chem. Res.* **2009**, *42*, 1995−2004.

(5) Proposed nonclassical H_2 binding in a paramagnetic metal complex: (a) Hetterscheid, D. G. H.; Hanna, B. S.; Schrock, R. R. *Inorg. Chem.* **2009**, *48*, 8569. (b) Kinney, R. A.; Hetterscheid, D. G. H.; Schrock, R. R.; Hoffman, B. M. *Inorg. Chem.* **2010**, *49*, 704. (c) Bart, S. C.; Lobkovsky, E.; Chirik, P. J. *J. Am. Chem. Soc.* **2004**, *126*, 13794. (d) Baya, M.; Houghton, J.; Daran, J.-C.; Poli, R.; Male, L.; Albinati, A.; Gutman, M. *Chem.—Eur. J.* **2007**, *13*, 5347.

(6) Lee, Y.; Kinney, R. A.; Hoffman, B. M.; Peters, J. C. *J. Am. Chem. Soc.* **2011**, *133*, 16366−16369.

(7) (a) Gadd, G. E.; Upmacis, R. K.; Poliakoff, M.; Turner, J. J. *J. Am. Chem. Soc.* **1986**, *108*, 2547−2552. (b) Bianchini, C.; Mealli, C.; Meli, A.; Bianchini, C.; Mealli, C.; Meli, A.; Peruzzini, M.; Zanobini, F. *J. Am. Chem. Soc.* **1988**, *110*, 8725−8726. (c) Heinekey, D.; Liegeois, A.; van Roon, M. *J. Am. Chem. Soc.* **1994**, *116*, 8388−8389. (d) Heinekey, D.; van Roon, M. *J. Am. Chem. Soc.* **1996**, *118*, 12134−12140. (e) Hebden, T. J.; St John, A. J.; Gusev, D. G.; Kaminsky, W.; Goldberg, K. I.; Heinekey, D. M. *Angew. Chem., Int. Ed.* **2010**, *50*, 1873−1876.

(8) Cobalt dihydrogen hydride complexes: (a) Sweany, R. L.; Russell, F. N. *Organometallics* **1988**, *7*, 719−727. (b) Doherty, M. D.; Grant, B.; White, P. S.; Brookhart, M. *Organometallics* **2007**, *26*, 5950−5960.

(9) A complex that is at least predominantly (if not fully) a dihydride in solution may be a dihydrogen complex in the solid state: Bianchini, C.; Mealli, C.; Peruzzini, M.; Zanobini, F. *J. Am. Chem. Soc.* **1992**, *114*, 5905−5906.

(10) Bontemps, S.; Bouhadir, G.; Dyer, P. W.; Miqueu, K.; Bourissou, D. *Inorg. Chem.* **2007**, *46*, 5149−5151.

(11) Whited, M. T.; Mankad, N. P.; Lee, Y.; Oblad, P. F.; Peters, J. C. *Inorg. Chem.* **2009**, *48*, 2507−2517.

(12) (a) Tsay, C.; Peters, J. C. *Chem. Sci.* **2012**, *3*, 1313. (b) Tsay, C.; Mankad, N. P.; Peters, J. C. *J. Am. Chem. Soc.* **2010**, *132*, 13975−13977.

(13) Greenwood, B. P.; Forman, S. I.; Rowe, G. T.; Chen, C.-H.; Foxman, B. M.; Thomas, C. M. *Inorg. Chem.* **2009**, *48*, 6251−6260.

(14) A study of the relationship between N_2 and H_2 binding in octahedral d^6 complexes: Morris, R. H.; Earl, K. A.; Luck, R. L.; Lazarowych, N. J.; Sella, A. *Inorg. Chem.* **1987**, *26*, 2674−2683.
(15) Rudd, P. A.; Liu, S.; Gagliardi, L.; Young, V. G., Jr.; Lu, C. C. *J. Am. Chem. Soc.* **2011**, *133*, 20724−20727.
(16) Morris, R. H. *Coor. Chem. Rev.* **2008**, *252*, 2381−2394.
(17) Sircoglou, M.; Bontemps, S.; Bouhadir, G.; Saffon, N.; Miqueu, K.; Gu, W.; Mercy, M.; Chen, C.-H.; Foxman, B. M.; Maron, L.; Ozerov, O. V.; Bourissou, D. *J. Am. Chem. Soc.* **2008**, *130*, 16729−16738.
(18) A search of the Cambridge Structural Database (including the Nov. 2011 update) reveals that the narrowest such ∠P−M−P is 139° (where M is a first-row metal and ∠P−M−P is bisected by a hydride).
(19) Harman, W. H.; Peters, J. C. *J. Am. Chem. Soc.* **2012**, *134*, 5080−5082.
(20) (a) Gonzalez, A. A.; Zhang, K.; Nolan, S. P.; Lopez de la Vega, R.; Mukerjee, S. L.; Hoff, C. D.; Kubas, G. J. *Organometallics* **1988**, *7*, 2429−2435. (b) Gonzalez, A. A.; Hoff, C. D. *Inorg. Chem.* **1989**, *28*, 4295−4297. (c) Hauger, B. E.; Gusev, D.; Caulton, K. G. *J. Am. Chem. Soc.* **1994**, *116*, 208−214. (d) Heinekey, D.; Voges, M. H.; Barnhart, D. M. *J. Am. Chem. Soc.* **1996**, *118*, 10792−10802. (e) Shen, J.; Haar, C. M.; Stevens, E. D.; Nolan, S. P. *J. Organomet. Chem.* **1998**, *571*, 205−213. (f) Grills, D. C.; van Eldik, R.; Muckerman, J. T.; Fujita, E. *J. Am. Chem. Soc.* **2006**, *128*, 15728−15741.
(21) The $(M−E)^n$ notation[22a,b] refers to the number of valence electrons, *n*, formally assigned to the metal (M = Fe, Co, or Ni) including those shared between the metal and the axially bound main group ligand (E = B or Si). Since the M−E bonds may be highly covalent and the M−E interactions are partially dictated by the cage structure of the tetradentate ligand and the M−E distance, the bonding electrons between M and E are often not reliably assigned to either atom.[22c,d] As such, the $(M−E)^n$ descriptor tracks the total number of valence electrons without implicit valence or oxidation number assignments
(22) (a) Hill, A. F. *Organometallics* **2006**, *25*, 4741−4743. (b) Parkin, G. *Organometallics* **2006**, *25*, 4744−4747. (c) Lee, Y.; Peters, J. C. *J. Am. Chem. Soc.* **2011**, *133*, 4438−4446. (d) Moret, M.-E.; Peters, J. C. *Angew. Chem., Int. Ed.* **2011**, *50*, 2063−2067.
(23) Whited, M. T.; Mankad, N. P.; Lee, Y.; Oblad, P. F.; Peters, J. C. *Inorg. Chem.* **2009**, *48*, 2507−2517.
(24) Bontemps, S.; Bouhadir, G.; Dyer, P. W.; Miqueu, K.; Bourissou, D. *Inorg. Chem.* **2007**, *46*, 5149−5151.
(25) Sheldrick, G. M. *SHELXTL 2000*; Universität Göttingen: Göttingen, Germany, 2000.
(26) Geometry optimized at the the B3LYP/6-31G(d) level using *Gaussian03*, revision D.01; Frisch, M. J. et al. Gaussian, Inc.: Wallingford, CT, 2004. Full reference in Supporting Information as ref 1.
(27) Brunner, E. *J. Chem. Eng. Data* **1985**, *30*, 269−273.
(28) McLinden, M. O.; Splett, J. D. *J. Res. Natl. Inst. Stand. Technol.* **2008**, *113*, 29−67.
(29) Jabloniec, A.; Horstmann, S.; Gmehling, J. *Ind. Eng. Chem. Res.* **2007**, *46*, 4654−4659.